Actinide and lanthanide speciation with high-energy resolution X-ray techniques

T. Vitova, M. A. Denecke, J. Goettlicher, K. Jorissen, J. J. Kas, K. Kvashnina, T. Pruessmann, J. J. Rehr, J. Rothe

Journal of Physics: Conference Series **430** (2013) 012117 doi:10.1088/1742-6596/430/1/012117

Actinide and lanthanide speciation with high-energy resolution X-ray techniques

T Vitova[1], M A Denecke[1], J Göttlicher[2], K Jorissen[3], J J Kas[3], K Kvashnina[4], T Prüßmann[1], J J Rehr[3] and J Rothe[1]

[1]Karlsruhe Institute of Technology, Institute for Nuclear Waste Disposal, P.O. Box 3640, D-76021 Karlsruhe, Germany

[2]Karlsruhe Institute of Technology, Institute for Synchrotron Radiation, P.O. Box 3640, D-76021 Karlsruhe, Germany

[3]Department of Physics, University of Washington, Seattle, WA 98195, USA

[4]European Synchrotron Radiation Facility (ESRF), 6 Rue Jules Horowitz, BP 220, 38043 Grenoble Cedex 9, France

E-mail: Tonya.Vitova@kit.edu

Abstract. High-energy resolution X-ray absorption spectroscopy (HR-XAS) and Resonant inelastic X-ray scattering (RIXS) combined with quantum theoretical tools are gaining importance for understanding electronic and coordination structures of actinide (An) and lanthanide (Ln) materials. HR-XAS is successfully used to remove lifetime broadening by registering the partial fluorescence yield emitted by the sample, thereby yielding highly resolved X-ray absorption near edge structure spectra (HR-XANES), which often display resonant features not observed in conventional XANES. We demonstrate the structural characterization capabilities of these novel techniques by comparative discussion of U M_4/L_3-HR-XANES and L_3-valence band RIXS (L_3-VB-RIXS) spectra of two model U(VI) minerals. We show that the *ab initio* multiple scattering theory based code *FEFF9.5* is an effective tool for calculations of An and Ln L_3-HR-XANES and L_3-RIXS spectra as it successfully reproduces dipole and quadrupole transitions in the same spectrum.

1. Introduction

High-energy resolution X-ray absorption near edge structure spectroscopy (HR-XANES) at the actinide (An), lanthanide (Ln) L_3 edge and An $M_{4,5}$ as well as An/Ln L_3 valence-band and core-to-core resonant inelastic X-ray scattering (VB-RIXS, CC-RIXS) are currently developing techniques providing new insights into the An and Ln electronic structure [1,2]. The highly efficient X-ray emission spectrometers developed in the last years minimise the experimental spectral broadening to values significantly smaller than the core-hole lifetime broadening and thereby approach the energy resolution limit for HR-XANES spectra [3]. These instruments are based mostly on an array of bent analyser crystals in a Rowland circle geometry diffracting and focusing the fluorescence onto a detector and, for example, resolve pre-edge structures in Ln and U L_3 edge HR-XANES (L_3-HR-XANES) spectra [1,2]. Only few HR-XANES for U materials have been reported so far and the U pre-edge is clearly visible in U(VI) spectra [1]. This spectral resonance is interpreted as resulting from $2p_{3/2} \rightarrow 5f$ electronic transitions, as corroborated by calculations with the *FDMNES* code. However, the calculated energy difference between the pre-edge and most intense resonance (white line, WL) is

smaller (4.5 eV) than the experimental one (7 eV) [1]. We present calculations with the *ab initio FEFF9.5* code [4], which agree well with the experimental spectrum. Additionally, we demonstrate that *FEFF9.5* is able to calculate the pre-edge ($2p_{3/2}\rightarrow 4f/5f$) and the WL ($2p_{3/2}\rightarrow 5d/6d$) in both the An/Ln L_3-HR-XANES and Ln L_3-CC-RIXS spectra, whereas other theoretical approaches calculate these absorption resonances separately [2]. The capability of the HR-XANES technique to measure the relative energy difference between An/Ln *f* and *d* states in a system of materials with small structural variations is extremely valuable for tuning theoretical approaches. It will also shed light onto the degree of stabilisation of the An *5f* valence orbitals across the actinide series and onto the amount of mixing in molecular orbitals between An/Ln valence with ligand orbitals. We also compare and discuss the sensitivity of the U L_3/M_4-HR-XANES and L_3-VB-RIXS to geometric structural changes for the same U(VI) oxidation state.

2. Experimental part and calculation details

The U L_3/M_4-HR-XANES, L_3-VB-RIXS of $Ca(UO_2)_2(PO_4)2{\cdot}10\text{-}12(H_2O)$ (meta-autunite), $NaCa_3(UO_2)(CO_3)_3(SO_4)F{\cdot}10(H_2O)$ (schroeckingerite) and Yb L_3-HR-XANES, L_3-CC-RIXS of Yb_2O_3 were recorded at the ID26 beamline, ESRF, Grenoble [3]. The synchrotron radiation was monochromatized by a Si(311) (U L_3 17166 eV, Yb L_3 8944 eV)/Si(111) (U M_4 3728 eV) double crystal monochromator (DCM). The experimental energy resolution was about 1.8 eV (U L_3), 0.8 eV (U M_4) or 1.2 eV (Yb L_3), measured as the width of the quasi-elastic peak. For each excitation energy, the emitted photons from the sample were diffracted by spherically bent Ge(777) (U $L\alpha_1$ 13614 eV), Si(220) (U M_β 3339.8 eV) or Si(620) (Yb $L\alpha_1$ 7416 eV) analyzer crystals and focused onto a X-ray silicon drift detector (SDD KETEK). The sample, crystal and detector were positioned in Rowland circle geometry with 1m diameter, equal to the bending radius of the crystals. The conventional fluorescence mode U M_4-XANES of $(UO_2)_8O_2(OH)_{12}{\cdot}12H_2O$ (schoepite) was recorded at the INE-Beamline, ANKA, Karlsruhe [5] using a pair of Si(111) crystals in the DCM and detecting U M_β fluorescence with a photo diode. The U/Yb L_3-HR-XANES and Yb L_3-CC-RIXS calculations were performed with the *ab initio* multiple-scattering (MS) theory based *FEFF9.5* code [4]. The atomic potentials were calculated self consistently on a cluster of 260 (U)/100 (Yb) atoms in the presence of a core-hole (U)/RPA (Yb) [4]. The exchange correlation Hedin-Lundquist potential was employed, reducing the $2p_{3/2}$ core-hole lifetime broadening (U: 8.1 eV, Yb: 4.3 eV) to 2.8 eV (U)/2 eV (Yb) and correcting the Fermi energy by -1 eV (U)/-8 eV(Yb). Full MS calculations were done on a cluster of 250 (U)/100 (Yb) atoms. Dipole ($2p_{3/2}\rightarrow 5d/6d$) and quadrupole transitions ($2p_{3/2}\rightarrow 4f/5f$) were taken into account. The Yb L_3-CC-RIXS calculations were performed by using the RIXS card (see [6]).

3. Results and discussion

The calculated spectra of Yb L_3-HR-XANES, L_3-CC-RIXS of Yb_2O_3 and U L_3-HR-XANES, U unoccupied *f* and *d* angular momentum projected density of states (*d* and *f*-DOS) of schroeckingerite are plotted in figure 1 a, b and figure 2 d. The *FEFF9.5* code successfully reproduces all spectral features at correct energy positions for U and at positions differing within few eVs from the experiment for Yb; some intensity differences are also observed. Yb_2O_3 characterises with Yb1 and Yb2 sites in octahedral and distorted octahedral local coordination environment, respectively (ICSD 163730). The weighted Yb1 and Yb2 calculated spectra including only dipole or quadruple transitions are shown in figure 1 a. The Yb L_3-HR-XANES spectrum is a linear combination of the two calculated spectra (1/4 Yb1 and 3/4 Yb2). The A region from the pre-edge structure originates mainly from $2p_{3/2}\rightarrow 4f$ electronic transitions but $2p_{3/2}\rightarrow 5d$ transitions are also well distinguishable. The energy difference between features A and B2 (13.4 eV) is equal, whereas between B1 and B2 (2.8 eV) and B2 and C (12.1 eV) is smaller than in the experimental spectrum (B2-A=13.4 eV, B2–B1=3.3 eV, C-B2=16.7 eV). The Yb $L\alpha_1$ on the energy transfer scale is plotted as a function of the excitation energy in figure 1 b (Yb L_3-CC-RIXS). The Yb_2O_3 L_3-CC-RIXS has intense pre-edge structure at about 8935 eV and a double structure in the WL region. The left RIXS plot shows the *FEFF9.5* calculation result using only dipole transitions ($2p_{3/2}\rightarrow 5d$), the middle plot the result obtained including quadrupole

transitions (*$2p_{3/2}$→4f*). The pre-edge absorption resonance is weak in the left plot (not visible on this scale) but has higher intensity and position comparable to the experimental spectrum (right) in the middle plot suggesting *$2p_{3/2}$→4f* dominates but mixes with *$2p_{3/2}$→5d* transitions in this part of the spectrum. This result partially confirms previous atomic multiplet calculations attributing the pre-edge to *$2p_{3/2}$→4f* electronic transitions, which however calculated only the pre-edge structure [2]. In case of uranium, *$2p_{3/2}$* electronic transitions to *5f* valence states contribute to the pre-edge region at about -9 eV, as at this energy the U *f*-DOS has large intensity (see figure 2 d). The WL and post-edge regions of the U L_3-HR-XANES spectrum is well described by dipole *$2p_{3/2}$→6d* transitions and resemble the U *d*-DOS as expected.

We use two U(VI) minerals, meta-autunite and schroeckingerite, to compare the structural sensitivity of U M_4/L_3-HR-XANES and U L_3-VB-RIXS spectra. Meta-autunite and schroeckingerite possess tetragonal (P4/nmm) (ICSD 20378) and triclinic (P -1) (AMCSD 0015705) crystal structures, respectively. In both mineral phases $U(VI)O_2^{2+}$ dioxo cations are coordinated solely by O atoms in the equatorial plane (figure. 2c,g). Second coordination neighbours are P/O atoms (meta-autunite) or C atoms (schroeckingerite). In figure 2a, the meta-autunite and schroeckingerite U L_3-HR-XANES spectra (2a top) are compared to their conventional fluorescence XANES spectra (2a bottom). All U L_3-HR-XANES features are sharper than in the conventional XANES and an additional pre-edge feature A is resolved. The U M_4-HR-XANES of these minerals also exhibit significantly improved energy resolution (figure 2f) which is shown here for schoepite where the distinct fine structure in the M_4-HR-XANES, is not resolved in the conventional fluorescence XANES (figure 2e). Only subtle differences between the mineral phases are observed in their U M_4-HR-XANES spectra such as the energy shift of feature D (figure. 2f inset). In contrast, the different U coordination environments in these mineral structures are clearly reflected in distinct variations of their U L_3-HR-XANES features. The An $M_{4,5}$-edges are of special interest as they directly probe unoccupied An *5f* electronic state densities (*3d→5f* transitions) and potentially can reveal subtle bonding differences such as metal-to-ligand charge donation. In addition, An M_4-XANES is expected to be especially useful for An speciation, since the reduced core-hole life-time broadening at the M_4 edge compared to the L_3 edge theoretically sharpens spectral features, thereby facilitating detection of minority valence species in oxidation state mixtures. However, our results on these two minerals indicate that the An L_3 edge might be more sensitive to changes in coordination environment for the same An oxidation state. For example, feature C in the U L_3-HR-XANES spectrum is an indicator for the U-O axial distance and shifts to lower energy upon lengthening of one or both U-O axial bonds [1]. The longest U-O axial distance in meta-autunite is about 0.2 Å longer than in schroeckingerite; however, feature C does not shift detectable to lower energies (figure. 2a). The U L_3-HR-XANES spectrum of schroeckingerite is calculated by elongation of the U-O1 bond from 1.8 to 2.5 Å compared to the spectrum of the unmodified structure in figure 2 h. Moreover, the pre-edge feature A has higher intensity, whereas the intensity of the WL (feature B) decreases. This trend is also visible in the experimental spectrum of meta-autunite compared to schroeckingerite. Notice that the reduction of WL intensity is stronger in the experiment than in the calculation, suggesting influence of additional structural effects. Nevertheless, this simulation implies that features A, B and C in L_3-HR-XANES can assist characterizing U-O bond distances more effectively than conventional XANES or M_4-HR studies.

Figure 1 b shows the U L_3-VB-RIXS spectra on the energy transfer scale of meta-autunite and schroeckingerite measured at an excitation energy at the maximum of the U L_3-HR-XANES WL (17176 eV). The intense peak at 0 eV is due to the elastically scattered incident photons. In the final state, the excited U atom has an electron promoted to an empty *6d* states and a core-hole in the filled part of the VB; this mimics a direct excitation from the VB [7]. Therefore, the U L_3-VB-RIXS spectrum, with maximum at about 12.7 eV, describes unoccupied *6d* states. The energy difference between the elastic peak and the VB-RIXS spectrum measures the energy gap between the highest occupied state and the lowest unoccupied valence state [7]. The U L_3-VB-RIXS of meta-autunite exhibits a broader VB feature compared to schroeckingerite, suggesting a larger energy spread of *6d* states and maybe less mixing with ligand valence orbitals. Comparison of the U L_3-HR-XANES WL

areas, which is proportional to the oscillatory strength of $2p_{2/3}$ electronic transitions to U *6d* states, corroborates this interpretation; the U *d* states in the U L_3-HR-XANES of meta-autunite have larger energy spread than schroeckingerite. Attempts to quantify this difference by fitting the U L_3-HR-XANES remain unsuccessful, as no unique model using Pseudo Voigt functions was found.

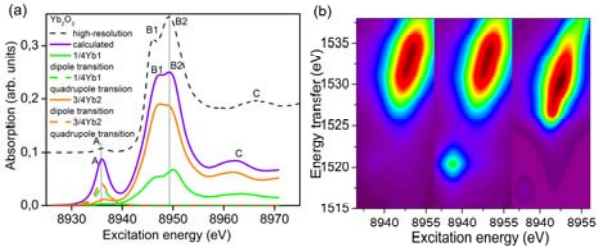

Figure 1. (a) Yb L_3-HR-XANES and calculation, (b) calculation including dipole (left) or dipole and quadrupole (middle) transitions, Yb L_3-CC-RIXS (right) of Yb_2O_3.

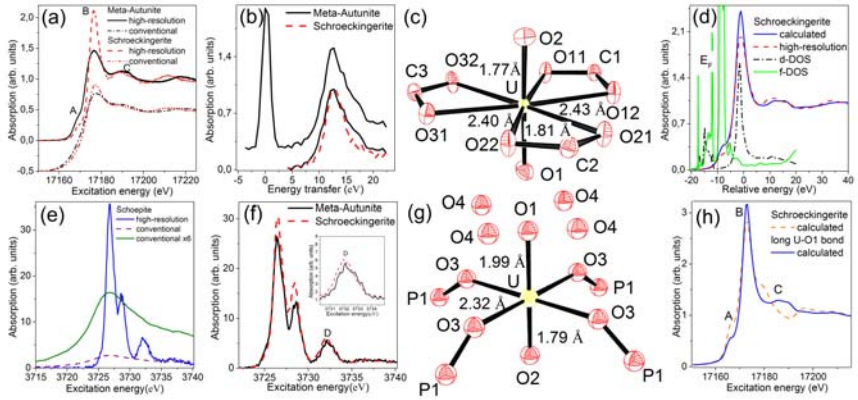

Figure 2. (a) U L_3-HR and -XANES, (b) U L_3-VB-RIXS, 3.6 Å atomic cluster for schroeckingerite (c) and meta-autunite (g), (d) U L_3-HR-XANES and (h) calculation for schroeckingerite, (e) U M_4-HR and -XANES for schoepite, (f) U M_4-HR-XANES of meta-autunite and schroeckingerite.

4. Conclusions

The *FEFF9.5* code emerges as a very useful tool for calculations of An/Ln L_3-HR-XANES and RIXS spectra, as it successfully reproduces all spectral features in both. The U(VI) L_3-HR-XANES spectra tend to be more sensitive to changes in geometric structure compared to U M_4-HR-XANES and VB-RIXS for the same U oxidation state. However, the techniques are complimentary and coupled to *ab initio* quantum chemical calculations provide detailed geometric and electronic structural information, which, e.g., can help to explain reduction mechanisms of Ln(III) to Ln(II) and can also be valuable for understanding the selectivity of N-donor ligands to complex An(III) over Ln(III) ions relevant for the separation and transmutation strategy for reduction the radiotoxicity of spent nuclear fuel.

Acknowledgments: We gratefully acknowledge KIT and the Helmholtz Association of German Research Centers for the financial support (VH-NG-734). We thank ESRF and ANKA for the granted beamtime.

References

[1] Vitova T *et al*. 2010 *PRB* **82** 235118
[2] Kvashnina K O, Butorin S M and Glatzel P 2011 *J. Anal. At. Spectrom.* **26** 1265
[3] Glatzel P and Bergmann U 2005 *Coord. Chem. Rev.* **249** 65
[4] Rehr J J, Kas J J, Prange M P, Sorini A P, Takimoto Y and Vila F 2009 *C. R. Physique* **10** 548 59
[5] Rothe J *et al.* 2012 *Rev. Sci. Instrum.* **83** 043105
[6] Kas J J, Rehr J J, Soininen J A, and Glatzel P 2011 *PRB* **83** 235114
[7] Glatzel P, Singh J, Kvashnina K O and van Bokhoven J A 2012 *JACS* **132** 2557